



Valence Connectivity Indices and Shape Indices Based Study of Testosterone Derivatives as SHBG Ligand

Singh R.K.* and Khan Mohd. Adil

Department of Chemistry, M.L.K. P.G. College, Balrampur, UP, INDIA

Available online at: www.isca.in

Received 22nd March 2013, revised 31st March 2013, accepted 6th April 2013

Abstract

Six descriptors namely shape indices (of order 1, 2 and 3) and valence connectivity indices (of order 0, 1 and 2) of forty SHBG binding testosterone derivatives have been calculated with the help of CAChe Pro of Fujitsu software using the semiempirical PM3 Hamiltonian. Observed biological activities of all forty compounds are in terms of pKd (SHBG-ligand dissociation parameter). These six descriptors have been used in deriving regression models. Shape indices (of order 1, 2 and 3) appear good descriptors for QSAR study of testosterone derivatives. Among these three descriptors, shape index (of order 3) is the best. The top five QSAR models developed from these descriptors have high predictive power and can be used to find out the SHBG activity of any new derivative of testosterone. The quality of regression has been adjudged by correlation coefficient, cross validation coefficient and statistical parameters obtained from Smith's Statistical Package (version 2.80).

Keywords: Testosterone, SHBG, valence connectivity indices, shape indices.

Introduction

The sex steroid testosterone controls various aspects of sexual differentiation, gonadal development, and the growth and functional maturation of reproductive tissues¹. Sex steroids or their immediate precursors are produced in the steroidogenic cells of the gonads, adrenal glands and placenta, and are transported in the blood to their target tissues by several steroid-binding proteins². A plasma glycoprotein, known as sex hormone-binding globulin (SHBG), binds biologically active androgens and is found in the blood. Because of its very high ligand binding affinity, plasma SHBG is the major plasma transport protein for biologically active androgens and estrogens³. It is synthesized by liver cells and has a 7-day half life in circulation. Changes in the blood levels of SHBG influence their plasma distribution and access to target tissues and cells⁴. SHBG greatly influences the bioavailable testosterone level because it binds with high affinity to a large fraction of the testosterone in circulation. The most preferred ligand of SHBG is the androgen 5 α -dihydrotestosterone⁵. SHBG was shown to mediate hormone action by a hormone-SHBG membrane-receptor complex by the generation of the second messenger cAMP inside the cells. It has also been found that numerous human diseases such as endometrial cancer, ovarian dysfunction, male and female infertility, osteoporosis, diabetes, and cardiovascular diseases are associated with abnormal SHBG levels, implicating the protein as a prospective drug target⁶⁻⁸. QSAR study of SHBG binding compounds has successfully done by Cherkasov^{9,10}. A set of parameters called inductive descriptors, which quantify the inductive effect of the electronegative atoms in a molecule, has been used by them. Also such computational methods gained much importance and recently have been applied to different compounds¹¹⁻¹⁵.

In this paper, QSAR study of forty SHBG binding testosterone derivatives has been done with the help of shape indices of order 1, 2 and 3^{16,17} and valence connectivity indices of order 0, 1 and 2^{18,19}. Observed biological activities of all forty compounds are in terms of pKd (SHBG-ligand dissociation parameter) which is different from earlier studies²⁰⁻²².

Theory: The values of six descriptors have been derived by solving the relevant equations given below:

(i) Valence connectivity index (χ): This index, originally defined by Randic and subsequently refined by Kier and Hall, is a series of numbers designated by "order" and "subgraph type"^{23,24}. There are four subgraph types; path, cluster, path/cluster, and chain. These types emphasize different aspects of atom connectivity within a molecule, the amount of branching, ring structures present and flexibility. It is calculated from the hydrogen suppressed molecular graph and defined as follows,

$${}^m\chi^v = \sum_{i=1}^{N_s} \prod_{k=1}^{m+1} \left[\frac{1}{\delta_k^v} \right]^{1/2}$$

Where, $\delta_k^v = \frac{(Z_k^v - H_k)}{(Z_k - Z_k^v - 1)}$ - valence connectivity for the k-

th atom in the molecular graph, Z_k = the total number of electrons in the k-th atom, Z_k^v = the number of valence electrons in the k-th atom, H_k = the number of hydrogen atoms directly attached to the kth non-hydrogen atom, $m = 0$ - atomic valence connectivity indices (called order-0), $m = 1$ - one bond path valence connectivity indices (called order-1), $m = 2$ - two bond fragment valence connectivity indices (called order-2).

(ii) **Shape index (κ_n):** These indices compare the molecule graph with “minimal” and “maximal” graphs, where the meaning of “minimal” and “maximal” depends on the order “n”. This is intended to capture different aspects of the molecular shape. Kier was first to propose shape indices for molecular graphs, the so called kappa shape indices. The first order kappa shape index (1κ or κ_1) is given by,

$${}^1\kappa = \frac{A(A-1)^2}{({}^1P)^2}$$

Where, iP = Length of paths of bond length i in the hydrogen suppressed molecule and A is the number of non hydrogen atoms in the molecule.

The second order kappa shape index (2κ or κ_2) is given by

$${}^2\kappa = \frac{(A-1)(A-2)^2}{({}^2P)^2}$$

The third order kappa shape index (3κ or κ_3) is given by

$${}^3\kappa = \frac{(A-1)(A-3)^2}{({}^3P)^2} \quad \text{if } A \text{ is odd}$$

$${}^3\kappa = \frac{(A-3)(A-2)^2}{({}^3P)^2} \quad \text{if } A \text{ is even}$$

Material and Methods

Forty derivatives of testosterone that have been taken from literature are used as study material. These are listed in table-1 alongwith their observed biological activity in terms of SHBG-ligand dissociation parameter i.e. pKd. The parent skeleton structure of testosterone is shown in figure-1. The QSAR study of all the derivatives of testosterone has been made with the help of six descriptors given below; i. Valence connectivity index of order 0. (${}^0\chi$), ii. Valence connectivity index of order 1. (${}^1\chi$), iii. Valence connectivity index of order 2. (${}^2\chi$), iv. Shape index of order 1. (κ_1), v. Shape index of order 2. (κ_2), vi. Shape index of order 3. (κ_3)

The values of descriptors have been evaluated by solving the relevant equations given in theory. For QSAR prediction, the 3D modeling and geometry optimization of all the derivatives and evaluation of values of descriptors have been done with the help of CAChe Pro of Fujitsu software using the semiempirical PM3 Hamiltonian. The Project Leader program associated with CAChe Pro has been used for multi linear regression (MLR) analysis. The statistical parameters have been calculated by Smith's Statistical Package (version 2.80).

Results and Discussion

Forty derivatives of testosterone given in table-1 have been considered for QSAR study where biological activity has been reported in terms of SHBG-ligand dissociation parameter (pKd). The values of six descriptors along with their biological activities are given in table-2. For the development of QSAR

models multi linear regression (MLR) analysis has been performed using different combinations up to four descriptors. Compound no. - 31 and 32 are outlier in the MLR analysis. Three QSAR models with good predictive power have been found from single descriptors namely shape index of order 1, 2 and 3. The MLR equations for these three models are given below,

$\text{SinglePA1} = -0.51247 * \kappa_1 + 16.343$. $r^2 = 0.583013$, $rCV^2 = 0.559699$, Std. error = 0.1409, SEE = 0.7586, t-value = 7.0952, p-value=0, DOF = 0.5715.

$\text{SinglePA2} = -1.71965 * \kappa_2 + 17.1998$. $r^2 = 0.736069$, $rCV^2 = 0.709896$, Std. error = 0.0998, SEE = 0.6035, t-value = 10.0217, p-value=0, DOF = 0.7288.

$\text{SinglePA3} = -4.61117 * \kappa_3 + 18.0597$. $r^2 = 0.776952$, $rCV^2 = 0.770113$, Std. error = 0.0893, SEE = 0.5548, t-value = 11.1088, p-value=0, DOF = 0.7708.

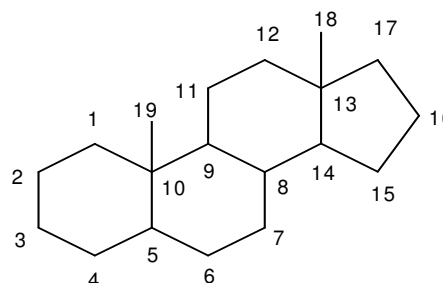


Figure-1
Parent Skeleton Structure of Testosterone

In the above regression equations, r^2 is correlation coefficient, rCV^2 is cross-validation coefficient, Std. Error is standard error, SEE is standard error of estimate and DOF is degrees of freedom. Shape indices appear important descriptors for this set of testosterone derivatives. All the above three models developed from single descriptor are good. Among these three models, QSAR model developed from shape index (of order 3) has the highest predictive power on the basis of value of correlation coefficient, cross-validation coefficient and statistical parameters. The trend of observed activity and predicted activity obtained from SinglePA3 is shown in figure-2. On the other hand, valence connectivity index of order 0, 1 and 2 individually fail to give reliable QSAR model. The predicted activities SinglePA1 , SinglePA2 and SinglePA3 , obtained by substituting the values of descriptor shown in table-2 in the above regression equations, are listed in table-3.

Various QSAR models, using descriptors in different combinations, have been developed but only top five models are reported. The best QSAR model (PA1) has been obtained by following regression equation,

$\text{PA1} = -0.578992 * \kappa_1 + 2.8754 * \kappa_2 - 9.9885 * \kappa_3 + 0.54334 * {}^0\chi + 15.9834$. $r^2 = 0.822955$, $rCV^2 = 0.782252$, Std. error = 0.0773, SEE = 0.4944, t-value = 12.9350, p-value=0, DOF = 0.8180.

Descriptors used in this QSAR model are shape index (order 1), shape index (order 2), shape index (order 3) and valence connectivity index (order 0). Value of correlation coefficient, cross-validation coefficient and statistical parameters indicate that the predictive power of this QSAR model is very good. The trend of observed activity and predicted activity obtained from PA1 is shown in figure-3.

The second best QSAR model (PA2) has been obtained by following regression equation,

$$PA2 = -0.27818 * \kappa_1 - 4.86353 * \kappa_3 + 0.82815 * {}^0\chi - 0.532034 * {}^2\chi + 16.0292. r^2 = 0.807879, rCV^2 = 0.740665, \text{Std. error} = 0.0813, \text{SEE} = 0.5150, t\text{-value} = 12.3037, p\text{-value} = 0, \text{DOF} = 0.8025.$$

This regression equation has been developed by using descriptors shape index (order 1), shape index (order-3), valence connectivity index (order-0) and valence connectivity index (order-2). Value of correlation coefficient, cross-validation coefficient and statistical parameters indicate that this model has good predictive power. The trend of observed activity and predicted activity obtained from PA2 is shown in figure-4.

The third best QSAR model (PA3) has been obtained by following regression equation,

$$PA3 = -0.333292 * \kappa_1 - 3.87646 * \kappa_3 + 0.801008 * {}^0\chi - 0.685657 * {}^1\chi + 16.7645. r^2 = 0.805092, rCV^2 = 0.724064, \text{Std. error} = 0.0820, \text{SEE} = 0.5187, t\text{-value} = 12.1939, p\text{-value} = 0, \text{DOF} = 0.7997.$$

This regression equation has been developed by using descriptors shape index (order 1), shape index (order-3), valence connectivity index (order-0) and valence connectivity index (order-1). Value of correlation coefficient, cross-validation coefficient and statistical parameters indicate that this model has good predictive power. The trend of observed activity and predicted activity obtained from PA3 is shown in figure-5.

The fourth best QSAR model (PA4) has been obtained by following regression equation,

$$PA4 = 0.808584 * \kappa_2 - 7.82536 * \kappa_3 + 0.478292 * {}^0\chi - 0.392411 * {}^2\chi + 17.4375. r^2 = 0.800686, rCV^2 = 0.764064, \text{Std. error} = 0.0831, \text{SEE} = 0.5245, t\text{-value} = 12.0268, p\text{-value} = 0, \text{DOF} = 0.7952.$$

Descriptors used in this QSAR model are shape index (order 2), shape index (order 3), valence connectivity index (order 0) and valence connectivity index (order 2). Value of correlation coefficient, cross-validation coefficient and statistical parameters indicate that the predictive power of this QSAR model is good. The trend of observed activity and predicted activity obtained from PA4 is shown in figure-6.

The fifth best QSAR model (PA5) has been obtained by following regression equation,

$$PA5 = -6.50984 * \kappa_3 + 0.524319 * {}^0\chi + 0.723604 * {}^1\chi - 0.908735 * {}^2\chi + 16.1207. r^2 = 0.800100, rCV^2 = 0.725212, \text{Std. error} = 0.0833, \text{SEE} = 0.5253, t\text{-value} = 12.0042, p\text{-value} = 0, \text{DOF} = 0.7946.$$

This regression equation has been developed by using descriptors shape index (order 3), valence connectivity index (order-0), valence connectivity index (order-1) and valence connectivity index (order-2). Value of correlation coefficient, cross-validation coefficient and statistical parameters indicate that this model has good predictive power. The trend of observed activity and predicted activity obtained from PA5 is shown in figure-7.

The predicted activities (PA1-PA5) obtained from above top five QSAR models are listed in table-4. From the values of correlation coefficient (r^2), cross-validation coefficient (rCV^2) and statistical parameters for the above five QSAR models, it is clear that the predictive power of all models is high and can be used to find out the SHBG activity of any derivative of testosterone. The correlation summary of top five QSAR models is presented in table-5.

Conclusion

It is clear from the above study that, the best combination of descriptors is shape index (order 1), shape index (order 2), shape index (order 3) and valence connectivity index (order 0) for QSAR study of testosterone derivatives as SHBG ligand. Three reliable QSAR models have been obtained from single descriptor namely shape index (order 1), shape index (order 2) and shape index (order 3). Whereas, valence connectivity indices (of order 0, 1 and 2) individually fail to give any reliable QSAR model. Therefore, shape indices of order 1, 2 and 3 appear good descriptor for QSAR study of testosterone derivatives. Among these three descriptors, shape index (order 3) is the best because the value of correlation coefficient is 0.776952 and value of cross-validation coefficient is 0.770113 for the QSAR model obtained from this descriptor. Also, shape index (order 3) is present in combination with other descriptors in all best five QSAR models.

References

1. Wilson J.D., Griffin J.E. and George F.W., Sexual differentiation: early hormone synthesis and action, *Biol. Reprod.* **22**, 9-17 (1980)
2. Westphal U., Steroid-Protein Interactions II, *Monographs on Endocrin* **27**, 603 (1986)
3. Dunn J.F., Nisula B.C. and Rodbard D., Transport of steroid hormones: binding of 21 endogenous steroids to both testosterone-binding globulin and corticosteroid-binding globulin in human plasma, *J. Clin. Endocrinol. Metab.* **53**, 58-68 (1981)

Table-1
Forty derivatives of testosterone with their biological activity in terms of SHBG-ligand dissociation parameter (pKd)

C. No.	Name of Compound	pKd
1	5- α -Dihydrotestosterone	9.74
2	1- α -methyl-Dihydrotestosterone	9.60
3	5-Androstene-19-nor-3 β ,17-diol	9.54
4	7 α -methyl-Dihydrotestosterone	9.38
5	2-Iodo Estradiol	9.32
6	4-methyl-Testosterone	9.31
7	Testosterone	9.20
8	5 α -Androstene-3 β , 17 β -diol	9.17
9	5 α -Androstane-3 α , 17 β -diol	9.11
10	2-Methoxy Estradiol	9.08
11	7 α -methyl-14-dehydro-19-Nor-testosterone	9.07
12	7 α -17-dimethyl-Dihydrotestosterone	9.05
13	7 α -methyl-5 α -Androstane-3 β , 17 β -diol	9.00
14	4-Androstene-3 β , 17 β -diol	9.00
15	Estradiol	8.83
16	17-methyl-Dihydrotestosterone	8.81
17	7 α , 17-dimethyl-Testosterone	8.76
18	6-dehydro-Estradiol	8.76
19	7 α -methyl-Testosterone	8.71
20	7-dehydro-Estradiol	8.62
21	17-methyl-1-Dihydrotestosterone	8.57
22	7 α , 17-dimethyl-5 α -Androstane-3 β , 17 β -diol	8.46
23	7 α -methyl-19-nor-Dihydrotestosterone	8.46
24	17-methyl-Testosterone	8.43
25	6 α -methyl-Testosterone	8.36
26	19-Nor-Dihydrotestosterone	8.36
27	7 α -methyl-1-dehydroTestosterone	8.36
28	17-Deoxoestrone	8.30
29	Estrone	8.18
30	16 α -hydroxyTestosterone	7.92
31	Dehydroepiandrosterone	7.84
32	Androstenedione	7.46
33	Deoxycortisol	7.44
34	Deoxycorticosterone	7.38
35	Pregnenolone	7.15
36	Cortisone	6.43
37	Corticosterone	6.34
38	Cortisol	6.20
39	Aldosterone	5.32
40	17 α -Aminopropyl-17 β -hydroxy-5 α -Androstan-3-one	4.96

Table-2
Values of descriptors and observed activities of forty derivatives of testosterone

C. No.	κ_1	κ_2	κ_3	${}^0\chi$	${}^1\chi$	${}^2\chi$	pKd
1	14.583	4.747	1.926	13.606	9.147	9.037	9.74
2	15.523	4.997	1.977	14.476	9.568	9.503	9.60
3	13.648	4.750	1.961	12.593	8.644	8.128	9.54
4	15.523	4.997	2.042	14.476	9.558	9.587	9.38
5	14.583	5.000	2.066	14.637	9.277	8.718	9.32
6	15.523	4.997	1.977	14.322	9.292	8.997	9.31
7	14.583	4.747	1.926	13.399	8.870	8.607	9.20
8	14.583	4.747	1.926	13.463	9.004	8.817	9.17
9	14.583	4.747	1.926	13.722	9.311	9.223	9.11
10	15.523	5.523	2.259	13.509	8.622	7.776	9.08
11	14.583	5.000	2.066	13.140	8.624	8.069	9.07
12	16.467	5.011	2.083	15.399	9.930	10.218	9.05
13	15.523	4.997	2.042	14.593	9.722	9.772	9.00
14	14.583	4.747	1.926	13.515	9.023	8.769	9.00
15	13.648	4.750	1.961	12.179	8.093	7.436	8.83
16	15.523	4.762	1.977	14.529	9.519	9.668	8.81
17	16.467	5.011	2.083	15.192	9.652	9.794	8.76
18	13.648	4.750	1.961	11.919	7.786	7.100	8.76
19	15.523	4.997	2.042	14.269	9.280	9.163	8.71
20	13.648	4.750	1.961	11.971	7.792	7.034	8.62
21	15.523	4.762	1.977	14.062	8.945	8.872	8.57
22	16.467	5.011	2.083	15.515	10.094	10.403	8.46
23	14.583	5.000	2.066	13.554	9.202	8.904	8.46
24	15.523	4.762	1.977	14.322	9.242	9.238	8.43
25	15.523	4.997	2.042	14.269	9.290	9.135	8.36
26	13.648	4.750	1.961	12.684	8.791	8.355	8.36
27	15.523	4.997	2.042	14.010	8.984	8.797	8.36
28	12.719	4.500	1.919	11.861	7.991	7.384	8.30
29	13.648	4.750	1.961	12.062	7.945	7.217	8.18
30	15.523	4.997	2.042	13.717	8.961	8.761	7.92
31	14.583	4.747	1.926	13.399	8.859	8.574	7.84
32	14.583	4.747	1.926	13.283	8.722	8.387	7.46
33	18.367	6.000	2.371	15.384	9.866	9.405	7.44
34	17.416	6.021	2.481	15.014	9.774	9.268	7.38
35	16.467	5.500	2.289	14.976	9.741	9.441	7.15
36	19.322	6.250	2.486	15.585	9.804	9.381	6.43
37	18.367	6.270	2.588	15.332	9.865	9.420	6.34
38	19.322	6.250	2.486	15.702	9.957	9.557	6.20
39	19.322	6.805	2.704	15.317	9.890	9.144	5.32
40	18.367	6.270	2.588	16.227	10.781	10.318	4.96

Where, κ_1 = Shape index (order 1), κ_2 = Shape index (order 2), κ_3 = Shape index (order 3), ${}^0\chi$ = Valence connectivity index (order 0), ${}^1\chi$ = Valence connectivity index (order 1), ${}^2\chi$ = Valence connectivity index (order 2).

Table-3
Predicted activities^{Single PA1 to Single PA3} of the testosterone derivatives

C. No.	Single PA1	Single PA2	Single PA3
1	8.870	9.037	9.179
2	8.388	8.607	8.943
3	9.349	9.031	9.017
4	8.388	8.607	8.644
5	8.870	8.602	8.533
6	8.388	8.607	8.943
7	8.870	9.037	9.179
8	8.870	9.037	9.179
9	8.870	9.037	9.179
10	8.388	7.702	7.643
11	8.870	8.602	8.533
12	7.904	8.583	8.455
13	8.388	8.607	8.644
14	8.870	9.037	9.179
15	9.349	9.031	9.017
16	8.388	9.011	8.943
17	7.904	8.583	8.455
18	9.349	9.031	9.017
19	8.388	8.607	8.644
20	9.349	9.031	9.017
21	8.388	9.011	8.943
22	7.904	8.583	8.455
23	8.870	8.602	8.533
24	8.388	9.011	8.943
25	8.388	8.607	8.644
26	9.349	9.031	9.017
27	8.388	8.607	8.644
28	9.825	9.461	9.211
29	9.349	9.031	9.017
30	8.388	8.607	8.644
33	6.930	6.882	7.127
34	7.418	6.846	6.619
35	7.904	7.742	7.505
36	6.441	6.452	6.596
37	6.930	6.418	6.126
38	6.441	6.452	6.596
39	6.441	5.498	5.591
40	6.930	6.418	6.126

Table-4
Predicted activities PA1 to PA5 of the testosterone derivatives

C. No.	PA1	PA2	PA3	PA4	PA5
1	9.344	9.065	9.065	9.166	9.123
2	9.482	9.028	8.962	9.202	9.129
3	8.994	8.800	8.774	8.766	8.826
4	8.833	8.667	8.717	8.660	8.622
5	9.234	9.408	9.259	8.893	9.136
6	9.399	9.170	9.028	9.327	9.308
7	9.232	9.122	9.089	9.235	9.205
8	9.267	9.064	9.048	9.184	9.145
9	9.407	9.062	9.045	9.148	9.134
10	7.652	7.775	7.743	7.636	7.671
11	8.420	8.513	8.507	8.432	8.469
12	8.419	8.634	8.728	8.545	8.535
13	8.897	8.666	8.698	8.644	8.634
14	9.295	9.132	9.077	9.227	9.229
15	8.769	8.825	8.820	8.840	8.839
16	8.835	8.984	9.038	8.972	8.971
17	8.306	8.688	8.752	8.612	8.610
18	8.628	8.788	8.823	8.847	8.786
19	8.720	8.721	8.742	8.728	8.697
20	8.656	8.867	8.860	8.898	8.878
21	8.582	9.021	9.058	9.061	9.034
22	8.482	8.632	8.708	8.528	8.546
23	8.645	8.412	8.443	8.302	8.345
24	8.723	9.042	9.062	9.042	9.053
25	8.720	8.736	8.735	8.739	8.730
26	9.044	8.754	8.746	8.721	8.774
27	8.580	8.702	8.737	8.747	8.680
28	8.835	9.052	9.108	8.835	8.920
29	8.706	8.845	8.828	8.870	8.870
30	8.421	8.478	8.518	8.621	8.543
33	7.277	7.125	7.010	7.402	7.344
34	6.589	6.621	6.667	6.435	6.492
35	7.537	7.695	7.720	7.431	7.541
36	6.404	6.479	6.449	6.810	6.678
37	5.858	6.018	6.128	5.892	5.890
38	6.467	6.482	6.438	6.797	6.690
39	5.677	5.323	5.331	5.518	5.396
40	6.344	6.282	6.217	5.968	6.206

Table-5
Correlation Summary of best five QSAR models

S. No.	QSAR Model	r ²	rCV ²	Std. Error	SEE	t -value	P-value	DOF	VC
1	PA1	0.822955	0.782252	0.0773	0.4944	12.9350	0	0.8180	4
2	PA2	0.807879	0.740665	0.0813	0.5150	12.3037	0	0.8025	4
3	PA3	0.805092	0.724064	0.0820	0.5187	12.1939	0	0.7997	4
4	PA4	0.800686	0.764064	0.0831	0.5245	12.0268	0	0.7952	4
5	PA5	0.800100	0.725212	0.0833	0.5253	12.0042	0	0.7946	4

Where; r²=Correlation coefficient, rCV²=Cross-validation coefficient, Std. Error = Standard error, SEE=Standard error of estimate, DOF=Degrees of freedom, VC=Variable count

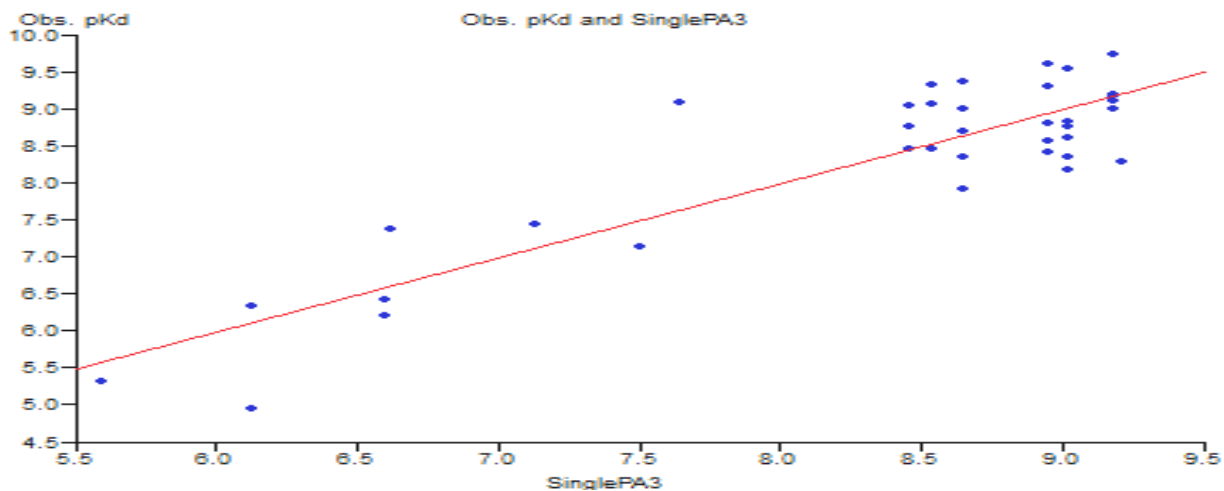


Figure-2

Trend of observed activity (pKd) and predicted activity (obtained from ^{Single}PA3) of the testosterone derivatives

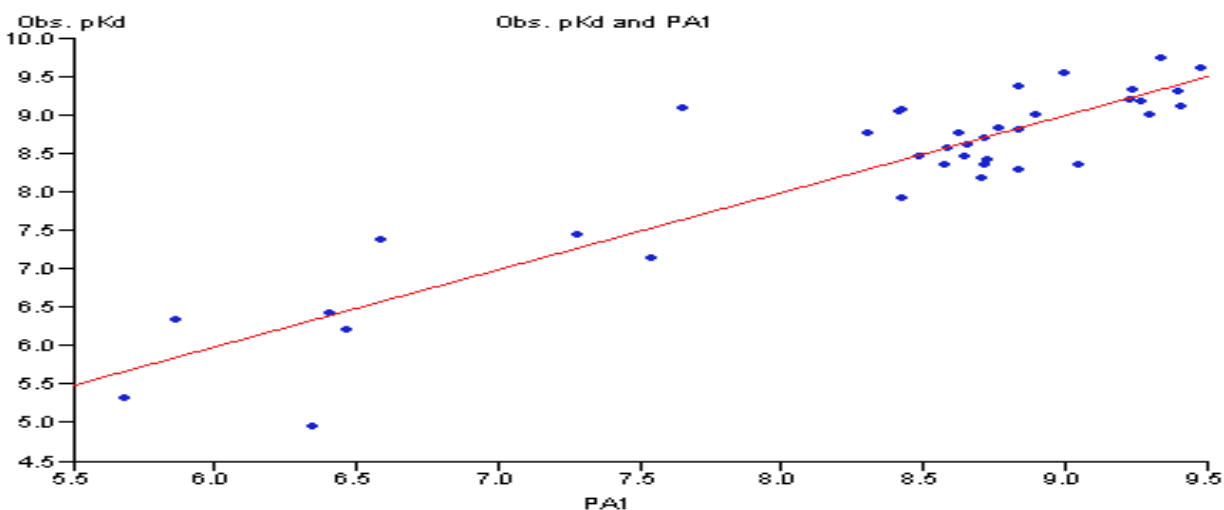


Figure-3

Trend of observed activity (pKd) and predicted activity (obtained from PA1) of the testosterone derivatives

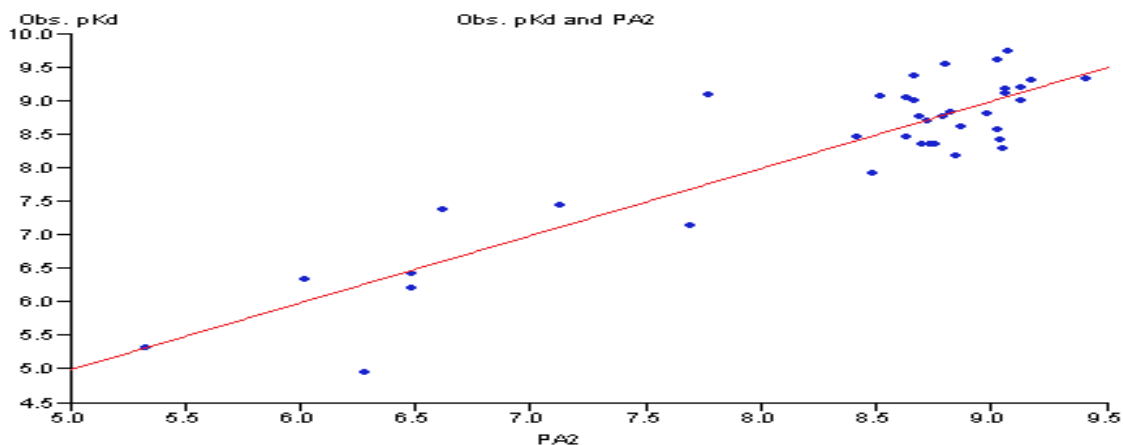


Figure-4

Trend of observed activity (pKd) and predicted activity (obtained from PA2) of the testosterone derivatives

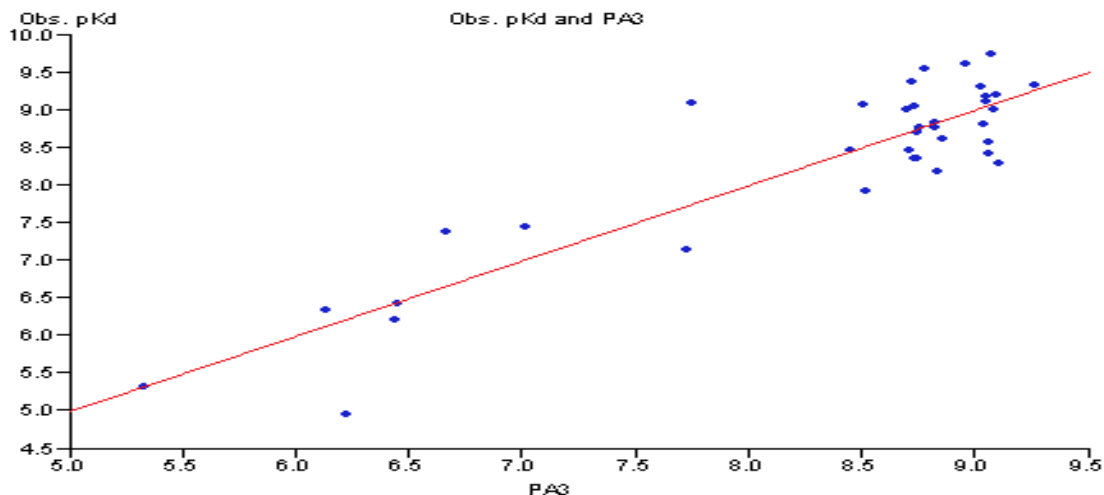


Figure-5
Trend of observed activity (pKd) and predicted activity (obtained from PA3) of the testosterone derivatives

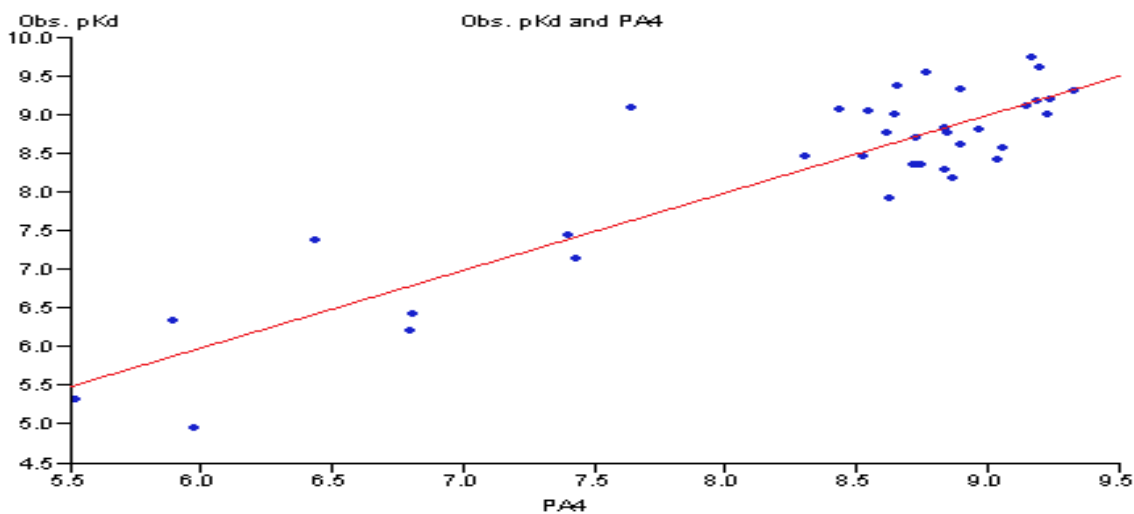


Figure-6
Trend of observed activity (pKd) and predicted activity (obtained from PA4) of the testosterone derivatives

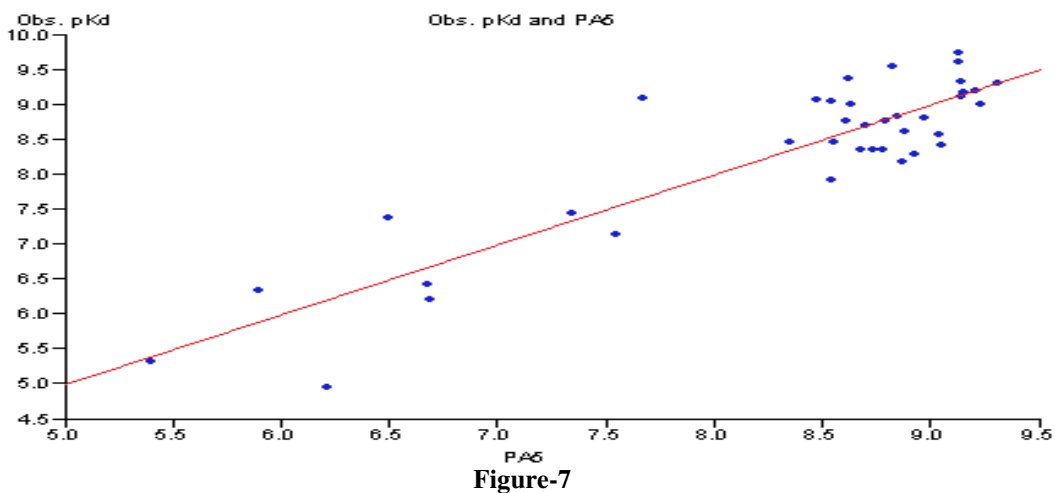


Figure-7
Trend of observed activity (pKd) and predicted activity (obtained from PA5) of the testosterone derivatives

4. Hammond G.L., Access of reproductive steroids to target tissues, *Obstet. Gynecol. Clin. North. Am.*, **29**, 411-423 (2002)
5. Hammond G.L. and Bocchinfuso W.P., Sex hormone-binding globulin/androgen-binding protein: steroid-binding and dimerization domains, *J. Steroid. Biochem. Mol. Biol.*, **53**, 543-552 (1995)
6. Hogeveen K.N., Cousin P., Pugeat M., Dewailly D., Soudan B. and Hammond G. L., Human sex hormone-binding globulin variants associated with hyperandrogenism and ovarian dysfunction, *J. Clin. Invest.*, **109**, 973-981 (2002)
7. Van Pottelbergh I., Goemaere S., Zmierczak H. and Kaufman J. M., Perturbed sex steroid status in men with idiopathic osteoporosis and their sons, *J. Clin. Endocrinol. Metab.*, **89**, 4949-4953 (2004)
8. Rapuri P.B., Gallagher J.C. and Haynatzki G., Endogenous levels of serum estradiol and sex hormone binding globulin determine bone mineral density, bone remodeling, the rate of bone loss, and response to treatment with estrogen in elderly women, *J. Clin. Endocrinol. Metab.*, **89**, 4954-4962 (2004)
9. Cherkasov A., Shi Z., Li Y., Jones S.J., Fallahi M. and Hammond G.L., Inductive charges on atoms in proteins: comparative docking with the extended steroid benchmark set and discovery of a novel SHBG ligand, *J. Chem. Inf. Model.*, **45**, 1842- 1853 (2005)
10. Cherkasov A., Inductive Descriptors. 10 Successful Years in QSAR, *Curt. Comp-Aided Drug Design*, **1**, 21-42 (2005)
11. Singh Rajeev, Kumar D., Singh Bhoop, Singh V.K. and Sharma Ranjana, Molecular structure, vibrational spectroscopic and HOMO, LUMO studies of S-2-picoyl- β -N-(2-acetylpyrrole) dithiocarbazate Schiff base by Quantum Chemical investigations, *Research Journal of Chemical Sciences*, **3(2)**, 79-84, (2013)
12. Gupta Y.K., Agarwal S.C., Madnawat S.P. and Ram Narain, Synthesis, Characterization and Antimicrobial Studies of Some Transition Metal Complexes of Schiff Bases, *Research Journal of Chemical Sciences*, **2(4)**, 68-71, (2012)
13. Buttrus H. Nabeel and Saeed T. Farah, Synthesis and Structural Studies on Some Transition metal complexes of Bis-(benzimidazole-2-thio) ethane, propane and butane ligands, *Research Journal of Chemical Sciences*, **2(6)**, 43-49, (2012)
14. Gupta Manish and Sharma Vimukta, Targeted drug delivery system: A Review, *Research Journal of Chemical Sciences*, **1 (2)**, (2011)
15. Glossman-Mitnik D., Computational Molecular Nanoscience: A Study of the Molecular Structure and Properties of a RAFT Polymerization Agent, *Research Journal of Chemical Sciences*, **1(9)**, 6-10, (2011)
16. Kier L. B., Shape indexes for orders one and three from molecular graphs, *Quant. Struct.-Act. Relat.*, **5**, 1-7 (1986)
17. Kier L.B., Indexes of molecular shape from chemical graphs, *Med. Res. Rev.* **7**, 417-440 (1987)
18. Randic M., On characterization of molecular branching, *J. Am. Chem. Soc.*, **97**, 6609-6615 (1975)
19. Kier L.B. and Hall L.H., Molecular Connectivity in Chemistry and Drug Research, Wiley, New York. (1986)
20. Singh P.P., Srivastava H.K. and Pasha F.A., DFT-based QSAR study of testosterone and its derivatives, *Bioorg. Med. Chem.*, **12**, 171 (2004)
21. Srivastava H.K., Pasha F.A. and Singh P.P., Atomic softness-based QSAR study of testosterone, *Int. J. Quant. Chem.* **103**, 237-245 (2005)
22. Srivastava H.K., Pasha F.A., Mishra S.K. and Singh P.P., Novel applications of atomic softness and QSAR study of testosterone derivatives, *Med. Chem. Res.*, **18**, 455-466 (2009)
23. Balaban A.T., Graph theory and theoretical chemistry, *Jour. of. Mol. Struc: THEOCHEM*, **120**, 117-142 (1985)
24. Petitjean M., Applications of the Radius-Diameter Diagram to the Classification of Topological and Geometrical Shapes of Chemical Compounds, *J. Chem. Inf. Comput. Sci.*, **32**, 331-337 (1992)